RESEARCH MEMORANDUM

for the

Bureau of Aeronautics, Department of the Navy

FLIGHT DETERMINATION OF THE LONGITUDINAL STABILITY CHARACTERISTICS OF A 0.133-SCALE ROCKET-POWERED MODEL OF THE CONSOLIDATED VULTEE XFY-1 AIRPLANE WITHOUT PROPELLERS AT MACH NUMBERS FROM 0.73 TO 1.19

TED NO. NACA DE 369

By Earl C. Hastings, Jr., and Grady L. Mitcham

Langley Aeronautical Laboratory
Langley Field, Va.

NATIONAL ADVISORY COMMITTEE
FOR AERONAUTICS
WASHINGTON

NACA RM SL54B03a

NATIONAL ADVISORY COMMITTEE FOR AERONAUTICS

RESEARCH MEMORANDUM

for the

Bureau of Aeronautics, Department of the Navy

FLIGHT DETERMINATION OF THE LONGITUDINAL STABILITY CHARACTERISTICS OF A 0.133-SCALE ROCKET-POWERED MODEL OF THE CONSOLIDATED VULTEE XFY-1 AIRPLANE WITHOUT PROPELLERS AT MACH NUMBERS FROM 0.73 TO 1.19

TED NO. NACA DE 369

By Earl C. Hastings, Jr., and Grady L. Mitcham

SUMMARY

A flight test has been conducted to determine the longitudinal stability and control characteristics of a 0.133-scale model of the Consolidated Vultee XFY-1 airplane without propellers for the Mach number range between 0.73 and 1.19.

The variation of lift-curve slope C_{L_α} with Mach number was gradual. Light buffet was encountered below a Mach number of 0.96. Mild wing dropping occurred at a Mach number of 0.91 for low values of lift coefficient.

The minimum drag coefficient was about 0.021 below a Mach number of 0.91, the point at which the drag rise began, and reached a maximum value of 0.099 at a Mach number of 1.18.

The high-lift pitching moments were nonlinear below a Mach number of 0.86 but all pitching moments were linear above this Mach number for the range of lift coefficients covered by the test.

The aerodynamic-center location moved gradually from its most forward location of 30.6-percent mean aerodynamic chord at Mach number 0.82 to its most rearward location at 50 percent mean aerodynamic chord at Mach number 1.05.

There was an abrupt decrease in pitch damping between Mach numbers of 0.935 and 0.995 followed by a gradual increase in damping to Mach number 1.17.

The transonic trim change was large and was in a nose-down direction.

The elevons were effective as a pitch control throughout the speed range of the test; however, at supersonic speeds, the effectiveness was reduced to about one-half its subsonic value.

INTRODUCTION

At the request of the Bureau of Aeronautics, Department of the Navy, the Langley Pilotless Aircraft Research Division is conducting tests to determine the drag and longitudinal and directional stability of the Consolidated Vultee XFY-1 airplane (phase III) at transonic and low supersonic speeds.

The Consolidated Vultee XFY-1 is a turboprop-powered, vertically rising interceptor, designed to fly at transonic speeds. The airplane has a low-aspect-ratio modified delta wing and vertical tail.

This paper presents the results from the first of a series of tests with 0.133-scale rocket-powered models. The primary purpose for the test of the model discussed herein was to determine the longitudinal stability and drag characteristics of the Consolidated Vultee XFY-1 airplane without propellers.

SYMBOLS

A	cross-sectional area, sq ft
a_l/g	longitudinal accelerometer reading
a_n/g	normal accelerometer reading
a_t/g	transverse accelerometer reading
b	wing span, ft
b_e	elevon span at trailing edge, ft
$\bar{c}$	wing mean aerodynamic chord, ft
$\bar{c}_e$	mean chord of elevon area back of hinge axis, ft
C_c	chord-force coefficient, positive in a rearward direction, $\frac{a_l}{g}\frac{W}{S}\frac{1}{q}$
C_D	drag coefficient, $C_N \sin \alpha + C_c \cos \alpha$

[redacted]

C_{D_b}	base-drag coefficient, $\frac{\Delta p}{q}\frac{\text{Base area}}{S}$
$C_{D_{min}}$	minimum drag coefficient
C_h	hinge-moment coefficient, $\frac{H}{qb_e\bar{c}_e^2}$
C_L	lift coefficient, $C_N \cos \alpha - C_c \sin \alpha$
C_{L_O}	lift coefficient at minimum drag
C_m	pitching-moment coefficient about center of gravity
C_{m_O}	pitching-moment coefficient about center of gravity at zero angle of attack and elevon deflection
$C_{m_q} + C_{m_{\dot{\alpha}}}$	pitch damping derivative
C_N	normal-force coefficient, positive toward top of model from model center line, $\frac{a_n}{g}\frac{W}{S}\frac{1}{q}$
g	acceleration due to gravity, 32.2 ft/sec^2
H	hinge moment, in-lb
I_Y	moment of inertia about pitch axis, slug-ft^2
$(L/D)_{max}$	maximum lift-drag ratio
l	length, ft
m	mass flow through duct, slugs/sec
m_o	mass of air flowing through a stream tube of area equal to inlet-cowl area under free-stream conditions, slugs/sec
M	Mach number
p	rolling velocity, radians/sec
P	period, sec

[redacted]

q	dynamic pressure, lb/sq ft
R	Reynolds number based on wing mean aerodynamic chord
r	radius of equivalent body of revolution, ft
S	wing area including body intercept, sq ft
$T_{1/2}$	time to damp to one-half amplitude, sec
V	velocity, ft/sec
W	weight of model, lb
x	station (measured from nose), ft
α	angle of attack at model center of gravity, deg
γ	flight-path angle, deg
δ	mean elevon deflection, positive, trailing edge down, deg
δ_p	recorded elevon deflection, positive, trailing edge down, deg
θ	angle between fuselage center line and horizontal, radians

Subscripts:

$q = \frac{d\theta}{dt}$

c.g. center-of-gravity location

$C_{m_q} = \frac{dC_m}{d\left(\frac{q\bar{c}}{2V}\right)}$

$\dot{\alpha} = \frac{1}{57.3}\frac{d\alpha}{dt}$

$C_{m_{\dot{\alpha}}} = \frac{dC_m}{d\left(\frac{\dot{\alpha}\bar{c}}{2V}\right)}$

Derivatives are expressed in this manner:

$$C_{L_\alpha} = \frac{\partial C_L}{\partial \alpha}, \quad C_{h_\delta} = \frac{\partial C_h}{\partial \delta}, \text{ and so forth}$$

MODEL AND APPARATUS

Model

A three-view drawing of the model tested in this investigation is given in figure 1 and the physical characteristics are given in table I. Figure 2 shows the area distribution and equivalent body of revolution for this configuration. This information is included for pressure drag correlation at a Mach number of 1.0. A photograph of the model is shown as figure 3.

The model had a modified delta wing with 57° sweepback of the leading edge and an aspect ratio of 1.85. The airfoil was a modified NACA 63-009 airfoil section at all spanwise stations. Gun pods and landing struts were located at each wing tip. Landing struts were also attached to the vertical fins.

Construction of the model was primarily of duralumin castings and fiber glass skin. The wing and vertical tails were duralumin plates and spars built up to the proper contour with laminated mahogany. The vertical fins had a leading-edge sweepback of 40° and the same airfoil section as the wing.

Longitudinal control was provided by two 9.25° swept constant-chord full-span elevons at the trailing edge of the wing. These elevons were actuated in flight by a pneumatic system designed to operate at about one complete square-wave cycle per second between the angles of -2° and -13° throughout the entire coasting phase of the flight.

Because of limited space inside the model, the internal ducting rearward of the inlets does not duplicate that of the full-scale airplane. An attempt was made however to duplicate the inlet-velocity-ratio conditions of the full-scale airplane by adding a minimum section at each duct exit.

Prior to the flight, the model was suspended by shock cords and shaken in the pitch plane with an electromagnetic shaker at frequencies up to 500 cycles per second to determine the natural frequencies of the model. Resonant frequencies occurred for the wing at 66, 105, 134, and 241 cycles per second. The node lines are shown in figure 4.

[redacted]

Since the base of the model tested was not geometrically similar to that of the full-scale airplane, it was necessary to determine the model base drag coefficient. Base drag was determined by surveying half of the base with seven static pressure tubes as shown in figure 5. These tubes were connected to small telemeter-type pressure sensing elements, the outputs of which were properly weighted and combined in a manner to yield electrical signals which were directly proportional to the average pressure over the integrated area. The model contained no sustainer rocket motor and was boosted to supersonic speeds by a solid-fuel 6.25-inch-diameter Deacon rocket motor. A photograph of the booster-model combination prior to launching is shown as figure 6. The data presented herein were obtained during the coasting portion of the flight after the model and booster had separated.

Apparatus

The model tested in this investigation was primarily instrumented to obtain longitudinal stability and drag data. Twelve channels of information were obtained by means of a telemeter system which recorded normal acceleration at the center of gravity and at the tail of the model, transverse and longitudinal accelerations at the center of gravity, and angle of attack and angle of yaw.

Other quantities recorded by the telemeter system were duct-exit total pressure, free-stream total pressure, model base pressure, angle-of-attack-vane base pressure, control position, and hinge moments.

Free-stream temperature and static pressure were obtained from a radiosonde released at time of firing. Ground apparatus consisted of a CW Doppler radar set and a radar tracking unit which was used to determine the model velocity and position in space.

ANALYSIS OF DATA

The data presented in this paper were obtained by reducing the data from a flight time history recorded during the flight. Free oscillations were created by pulsing the elevons in an approximate square-wave motion which resulted in changes in normal acceleration, angle of attack, and hinge moment. The analysis of these oscillations is based on two degrees of freedom, acceleration normal to the flight path, and rotation in pitch about the center of gravity. A more complete discussion of the methods and corrections used in reducing these data from the flight time history records to the parameters presented herein is given in the appendixes of references 1 and 2.

[redacted]

Since the angle-of-attack and angle-of-sideslip indicator was located ahead of the center of gravity, a correction to the indicated readings for flight-path curvature and rate of pitch was applied as in reference 3. The corrected values in conjunction with values of normal-force coefficient C_N and chord-force coefficient C_c were used to compute lift coefficient C_L and drag coefficient C_D.

Since the elevon angles recorded from the flight test were not read directly from the elevon but from a torque rod inboard of it, two corrections were applied to the recorded angles. The first was for the twist in the torque rod between the elevon and the control-position recorder. This twist was determined from a ground static test by applying known hinge moments to the elevon and measuring the angles at the control-position recorder and at the end of the torque rod. This difference in these angles was then the amount of twist in the torque rod due to a known hinge moment.

Elevon twist due to aerodynamic loading was determined by assuming a square elevon spanwise loading and determining the factor $\delta/\delta P$ from the relation

$$\frac{\Delta H}{\Delta \delta_P} = \frac{\delta}{\delta_P}\left(-\frac{b_e}{2}F - \frac{2.5}{b_e K_T} + \frac{2.5}{b_e K_T}\sqrt{-1.4 - 0.4 b_e^2 K_T F + 0.004 b_e^4 K_T^2 F^2 + 2.4\,\frac{\delta}{\delta_P}}\right)$$

where F is a function of out-of-trim hinge moment and hinge moment due to angle of attack and K_T is a factor determined by the elevon flexibility under known static hinge moments. This analytical equation is from an unpublished analysis.

These corrections, in conjunction with the recorded hinge-moment data, were used to correct the control positions recorded during the flight test to a mean spanwise value.

Pitching moments were determined by the use of normal accelerometers at the center of gravity and in the tail of the model. The difference in the two accelerometer readings is proportional to the angular acceleration in pitch by the following relation:

$$\ddot{\theta} = \frac{a_{n_{cg}} - a_{n_t}}{l}$$

where l is the distance in feet between the two accelerometers.

[redacted]

The total pitching-moment coefficients were then calculated and corrected for aerodynamic damping by the following equation:

$$C_m = \frac{I_Y \ddot{\theta}}{qS\bar{c}} - \left(C_{m_q} + C_{m_{\dot{\alpha}}}\right)\dot{\alpha} - C_{m_{\dot{\theta}}}\dot{\gamma}$$

The quantity $\dot{\alpha}$ was obtained by differentiating the measured α curve and the quantity $\dot{\gamma}$ was calculated from the measured accelerations at the model center of gravity, the gravity component being neglected.

ACCURACY

A discussion of the limitations of the technique and of the accuracy of the measured quantities is given in reference 4. In general, the possible instrument errors should be proportional to a certain percentage of the total calibrated range of the instrument. Estimated values of the maximum possible errors in C_L, C_D, and $pb/2V$ have been made based on the calibration ranges of the instruments used in this model. The probable error due to this source, however, may be less than the values estimated and presented in the following table:

M	ΔC_L	ΔC_D	$\Delta \frac{pb}{2V}$
0.75	±0.02	±0.004	±0.002
1.20	±.008	±.001	±.003

For this test, Mach number was available from two sources. Mach number was computed from the free-stream total pressure and from the CW Doppler radar set. At supersonic speeds, agreement between these two sources was better than ±1 percent and at subsonic speeds the difference in Mach number was less than ±2 percent. This same order of accuracy was predicted in reference 4.

The errors in the measured values of angles of attack and elevon deflections would be constant throughout the Mach number range of this test, since they are independent of dynamic pressure or velocity. The recorded elevon deflections should be accurate to about $\pm 0.2^\circ$ and angle of attack to about $\pm 0.3^\circ$. It should be pointed out, however, that the errors quoted above are systematic errors and will not change any of the values of slope. The random errors encountered can be seen by the scatter in the data.

RESULTS AND DISCUSSION

The Reynolds number range for this test is given as a function of Mach number in figure 7.

Lift

Lift-curve slope.- Figure 8 presents some typical curves of model lift coefficient plotted against angle of attack at various Mach numbers for the elevon angles used during the flight. These plots show the linearity of lift coefficient with angle of attack at each Mach number presented. For the range of lift coefficients and the Mach numbers covered, the lift was linear with angle of attack below $C_L = 0.32$; whereas the lift was nonlinear with angles of attack above $C_L = 0.32$.

The variation of lift-curve slope C_{L_α} with Mach number is shown in figure 9. These values were taken over the linear lift range for both the small and large elevon deflections. Results from tunnel tests of a model of the Consolidated Vultee XFY-1 (ref. 5) are plotted for comparison in figure 9. The agreement is generally considered to be good.

The values of lift-curve slope for $\delta \approx -2^\circ$ increase gradually with Mach number from a value of 0.051 at $M = 0.75$ to a maximum of 0.074 at $M = 0.98$ and then decrease gradually to a value of 0.058 at $M = 1.19$.

At subsonic speeds, changing the elevon angle from $\delta \approx -2^\circ$ to $\delta \approx -12^\circ$ reduces the values of lift-curve slope 0.005 at $M = 0.75$ and 0.013 at $M = 0.95$ whereas above $M = 0.95$ there are insufficient high-lift data to draw any definite conclusions.

Buffet.- The flight time history of the 0.133-scale Consolidated Vultee XFY-1 model showed the presence of some high-frequency oscillations in normal acceleration below $M = 0.96$ at the higher lift coefficients obtained. These oscillations are the result of flow separation over some portion of the model. The intensity rise of the buffet or flow separation occurred at $C_L = 0.19$ at $M = 0.96$. The maximum amplitude of these buffet oscillations corresponded to a ΔC_L of 0.044. Reduction of the C_L range to between 0 and 0.1 at $M = 0.91$ resulted in diminishing the amplitude of the buffet oscillations until they were within the accuracy of the instrumentation (which corresponded to $\Delta C_L = 0.015$ at $M = 0.9$). At $M = 0.88$ when the C_L range was increased to 0.45, the buffet intensity rise occurred at $C_L = 0.35$ with a maximum amplitude of $\Delta C_L = 0.06$. The buffet intensity rise occurred at $C_L = 0.45$ at $M = 0.8$.

The intensity rise as discussed in the preceding paragraph refers to the point at which an apparent abrupt increase in buffet intensity occurs. A section from the flight telemeter record which shows some of the buffet encountered is shown as figure 10. At $C_L = 0.2$ as indicated on the telemeter trace, the amplitudes of the buffet oscillations are much larger than those that are indicated in the telemeter trace where C_L is near 0. As a result of the large normal accelerations, it was necessary to use rather wide range accelerometers which resulted in reduced accuracy for small-amplitude oscillations. The accuracy of the instrument from which the buffet was determined amounted to a ΔC_L of 0.015. Also, as a result of the rapid control movement, it is sometimes difficult to determine the exact point where the small-amplitude oscillations begin.

Wing dropping.- Longitudinal and lateral control on the Consolidated Vultee XFY-1 airplane is provided by a single set of constant-chord control surfaces (elevons) on the wing trailing edge. Deflecting the elevons together provides longitudinal control whereas deflecting them differentially provides lateral control. For this test, there was no differential deflection of the elevons. The roll rate for the model, presented in figure 11 as wing-tip helix angle $pb/2V$ against Mach number, is within the accuracy of the measuring instrument (±1.5 radians/sec) throughout the Mach number range except at $M = 0.91$ where wing dropping was evident at low lift coefficients. The maximum rate of roll was about 4.3 radians/second; this value would correspond to only about 0.57 radian/second on the full-scale airplane.

Drag

The basic drag data for the 0.133-scale model of the Consolidated Vultee XFY-1 airplane with propellers off are presented in the form of lift-drag polars in figure 12. The Mach number values quoted in figure 12 represent an average value for $\Delta M \leq 0.02$. The effect of a small variation in Mach number on drag coefficient in the drag-rise region is evident in the trend of points shown in the polar for an average Mach number of 0.942.

Minimum drag.- The variations of the minimum drag coefficient $C_{D_{min}}$ and the lift coefficient at minimum drag C_{L_O} as determined from the drag polars of figure 12 are presented as a function of Mach number in figures 13 and 14, respectively. These values of $C_{D_{min}}$ include both internal and base drag. As the result of a malfunction in the instrumentation, measurements of internal drag were not obtained. An estimate of internal drag based on previous experience indicates the magnitude of the internal drag based on wing area to be in the order of 0.001. The

drag rise occurs at $M = 0.91$ with the elevon deflection at approximately -2.0°. The minimum drag coefficient $C_{D_{min}}$ is a constant value of about 0.021 from $M = 0.75$ to $M = 0.91$ with an abrupt increase to a value of 0.085 at $M = 1.0$ followed by a more gradual increase to 0.099 at $M = 1.18$. The values of $C_{D_{min}}$ for the larger elevon angles at subsonic speeds were determined by extrapolation of the curves in figure 12 since the model did not oscillate below $C_L = 0.1$.

As a result of the base area on the model being somewhat larger than on the full-scale airplane, the base pressure was measured in order to determine the base drag. The base drag $C_{D_{base}}$ which is very small is given as a function of Mach number in figure 13.

Variation of drag with lift.- The general quadratic expression used in this paper for drag as a function of lift due to angle of attack is of the form

$$C_D = C_{D_{min}} + \frac{dC_D}{d(\Delta C_L)^2}(C_L - C_{L_O})^2$$

where

$$\Delta C_L = C_L - C_{L_O}$$

The variation of $dC_D/d(\Delta C_L)^2$ with Mach number is presented in figure 15. The values of $dC_D/d(\Delta C_L)^2$ generally show the same trend and level with Mach number as the 6.5-percent-thick delta wing in reference 6. Also shown in figure 15 is a plot of the drag due to lift parameter $1/C_{L_\alpha}$. It would be expected, however, that the values of $dC_D/d(\Delta C_L)^2$ for the present test would be lower throughout the subsonic Mach number range since the thickness ratio was 9 percent as compared to 6.5 percent for the wing in reference 6. The level of $dC_D/d(\Delta C_L)^2$ for the present test when compared with tests of a thinner wing can probably be explained by flow separation over the rather blunt body and about the inlets. Values of $dC_D/d(\Delta C_L)^2$ for the larger elevator deflections are not presented since the model did not oscillate to $C_{D_{min}}$ as can be seen in figure 12. The elevon comprises a large percentage of the wing area and results in a substantial penalty in drag due to lift when large deflections are used. A more complete discussion on these effects can be found in reference 6.

[redacted]

Lift-drag ratio.- The maximum lift-drag ratios $(L/D)_{max}$ and the lift coefficient for $(L/D)_{max}$ are plotted as functions of Mach number in figures 16(a) and 16(b), respectively, for $\delta \approx -2.0^{\circ}$ and $\delta \approx -12.0^{\circ}$. Only two values of $(L/D)_{max}$ with $\delta \approx -2.0^{\circ}$ were obtained since at the other Mach numbers the maximum C_L attained was less than the C_L for $(L/D)_{max}$. At $M = 0.75$, changing the elevon deflection from $\delta \approx -2.0^{\circ}$ to $\delta \approx -12.0^{\circ}$ resulted in about a 30-percent reduction in $(L/D)_{max}$.

Hinge Moments

The hinge-moment characteristics of the elevon in the form of the variation of hinge-moment coefficient with elevon deflection C_{h_δ} and the variation of hinge-moment coefficient with angle of attack C_{h_α} are given as functions of Mach number in figures 17 and 18, respectively. The data indicate that C_h may be nonlinear with α above 10° from $M = 0.72$ (lower limit of test) to $M = 0.86$ above which the maximum value of angle of attack attained was less than 10°. There is also the possibility that C_{h_α} may be nonlinear with δ since the elevon was deflected in only two positions.

Static Longitudinal Stability

The basic pitching-moment data are shown in figure 19 as the variation of pitching-moment coefficient with lift coefficient. The values of total C_m presented in this figure were obtained by use of two normal accelerometers as discussed in the section "Analysis of Data." From $M = 0.86$ to $M = 1.19$, C_m varies linearily with C_L over the lift range covered for both small and large elevon deflections whereas, below $M = 0.86$, C_m is nonlinear with C_L for $\delta \approx -12^{\circ}$.

The periods of the short-period longitudinal oscillations in angle of attack resulting from the abrupt movement of the elevons are shown in figure 20. These values of period were used to calculate the longitudinal stability parameter C_{m_α} by the following relation

$$C_{m_\alpha} = -\frac{I_Y}{qS\bar{c}}\left[\frac{4\pi^2}{P^2} + \left(\frac{0.693}{T_{1/2}}\right)^2\right]$$

[redacted]

The values of C_{m_α} were divided by C_{L_α} and are shown plotted for comparative purposes in figure 19. This calculated method of determining dC_m/dC_L assumes linearities whereas the two-accelerometer method measures the total moment variation with angle of attack and lift coefficient.

The values of aerodynamic-center location presented in figure 21 were determined from the linear range of dC_m/dC_L (fig. 19). The aerodynamic center for $\delta \approx -2^\circ$ moves gradually from the most forward location of the 30.6-percent mean aerodynamic chord at $M = 0.82$ to the most rearward location of the 50.0-percent mean aerodynamic chord at $M = 1.05$.

Damping in Pitch

The damping-in-pitch characteristics of the model are given by the parameters $T_{1/2}$ (the time required to damp to half amplitude) and $C_{m_q} + C_{m_{\dot{\alpha}}}$ which are presented in figures 22 and 23, respectively. These parameters were determined from an analysis of the rate of decay of the transient short-period oscillations resulting from abrupt elevon movements. Figure 23 shows an abrupt increase in pitch damping between $M = 0.88$ and $M = 0.935$ followed by an abrupt decrease between $M = 0.935$ and $M = 0.995$, then an increase in damping between $M = 1.0$ and $M = 1.17$. This abrupt increase in damping followed by the abrupt loss and then an increase has been indicated for other triangular wings in reference 7 and unpublished rocket-powered model results.

Longitudinal Control Effectiveness

The effectiveness of the swept constant-chord full-span elevon in producing lift and pitching moments is given in figures 24 and 25. The lift coefficient per degree of elevon deflection C_{L_δ} remains nearly constant at a value of 0.0135 below a Mach number of about 0.95 and then decreases to a value of 0.0070 at $M = 1.12$.

Pitching-moment effectiveness C_{m_δ} varies gradually from -0.0075 at $M = 0.75$ to a value of -0.0032 at $M = 1.12$.

Two other longitudinal control effectiveness parameters, the change in trim angle of attack per degree of elevon deflection $(\Delta\alpha/\Delta\delta)_{trim}$ and the rate of change in trim lift coefficient with elevon deflection $\frac{\Delta C_{L_{trim}}}{\Delta\delta}$, are presented as functions of Mach number in figures 26

[redacted]

and 27. Both of these parameters show comparatively low values of control effectiveness at the higher speeds. This result is partially due to the rather large rearward movement of the aerodynamic-center location at supersonic speeds in addition to the reduction in control effectiveness.

The longitudinal control effectiveness parameters presented indicate that the elevon is an effective control for producing lift and pitching moments throughout the Mach number range of this test, although the effectiveness is reduced at the higher Mach numbers.

Longitudinal Trim

The basic pitching-moment coefficient C_{m_o} at zero angle of attack and zero elevon deflection is shown as a function of Mach number in figure 28. The trim change begins at approximately $M = 0.9$ with C_{m_o} remaining negative throughout the Mach number range covered by the test.

CONCLUSIONS

Results from the flight test of a 0.133-scale model of the Consolidated Vultee XFY-1 airplane without propellers from Mach number 0.73 to Mach number 1.19 indicate the following conclusions:

1. Lift-curve slope varies gradually with Mach number, a maximum value of 0.074 occurring at a Mach number of 0.98.

2. Light buffet was encountered below a Mach number of 0.96 and the intensity rise occurred at a lift coefficient of 0.19 at that Mach number.

3. Mild wing dropping occurred at Mach number of 0.91 with a maximum rate of roll corresponding to about 0.57 radian per second for the full-scale airplane.

4. The minimum drag coefficient for an elevon deflection of approximately -2.0° has a value of about 0.021 below about a Mach number 0.91, the point of drag rise with an abrupt increase to 0.085 at Mach number 1.0 followed by a more gradual increase to a value of 0.099 at a Mach number 1.18.

5. There is some nonlinearity in the pitching moments below a Mach number of 0.86 in the high-lift region whereas, from Mach number 0.86 to Mach number 1.19, the upper limit of the test, the pitching moments are linear over the range of lift coefficients covered.

6. The aerodynamic center with an elevon deflection of approximately -2.0° moves gradually from its most forward location of 30.6-percent mean aerodynamic chord at a Mach number of 0.82 to its most rearward location at 50-percent mean aerodynamic chord at a Mach number of 1.05.

7. There is an abrupt increase in pitch damping between Mach numbers of 0.88 and 0.935 followed by an abrupt loss in damping between Mach numbers 0.935 and 0.995, then a gradual increase in damping to a Mach number of 1.17.

8. The transonic trim change, a pitching-down tendency, is quite large; the pitching-moment coefficient at zero angle of attack and elevon deflection varies from a value of about -0.016 at a Mach number of 0.75 to a value of -0.072 at a Mach number of 1.0.

9. The elevon is an effective control in producing lift and pitching moment throughout the Mach number range covered by the test, although the effectiveness is reduced to about one-half of its subsonic value at supersonic speeds.

Langley Aeronautical Laboratory,
National Advisory Committee for Aeronautics,
Langley Field, Va., January 26, 1954.

Earl C. Hastings Jr.

Earl C. Hastings, Jr.
Aeronautical Research Scientist

Grady L. Mitcham

Grady L. Mitcham
Aeronautical Engineer

Approved: Joseph A. Shortal

Joseph A. Shortal
Chief of Pilotless Aircraft Research Division

ecc/lso

[redacted]

REFERENCES

1. Mitcham, Grady L., Stevens, Joseph E., and Norris, Harry P.: Aerodynamic Characteristics and Flying Qualities of a Tailless Triangular-Wing Airplane Configuration As Obtained From Flights of Rocket-Propelled Models at Transonic and Low Supersonic Speeds. NACA RM L9L07, 1950.

2. Gillis, Clarence L., Peck, Robert F., and Vitale, A. James: Preliminary Results From a Free-Flight Investigation at Transonic and Supersonic Speeds of the Longitudinal Stability and Control Characteristics of an Airplane Configuration with a Thin Straight Wing of Aspect Ratio 3. NACA RM L9K25a, 1950.

3. Mitchell, Jesse L., and Peck, Robert F.: An NACA Vane-Type Angle-of-Attack Indicator for Use at Subsonic and Supersonic Speeds. NACA RM L9F28a, 1949.

4. Gillis, Clarence L., and Vitale, A. James: Wing-On and Wing-Off Longitudinal Characteristics of an Airplane Configuration Having a Thin Unswept Tapered Wing of Aspect Ratio 3, As Obtained From Rocket-Propelled Models at Mach Numbers From 0.8 to 1.4. NACA RM L50K16, 1951.

5. Wall, P. J.: A Preliminary Analysis of the First Series of High-Speed Wind Tunnel Tests of the Convair Model 5 Airplane. Aero Memo No. A-5-27, Consolidated Vultee Aircraft Corp., Mar. 3, 1952.

6. Mitcham, Grady L., Crabill, Norman L., and Stevens, Joseph E.: Flight Determination of the Drag and Longitudinal Stability and Control Characteristics of a Rocket-Powered Model of a 60° Delta-Wing Airplane From Mach Numbers of 0.75 to 1.70. NACA RM L51I04, 1951.

7. Tobak, Murray: Damping in Pitch of Low-Aspect-Ratio Wings at Subsonic and Supersonic Speeds. NACA RM A52L04a, 1953.

[redacted]

TABLE I.- PHYSICAL CHARACTERISTICS OF A 0.133-SCALE MODEL OF THE CONSOLIDATED VULTEE XFY-1 AIRPLANE

Wing:	
Area (included), sq ft	6.31
Theoretical span, ft	3.42
Aspect ratio (based on theoretical span)	1.85
Mean aerodynamic chord, ft	2.09
Sweepback of leading edge, deg	57
Sweepback of trailing edge, deg	9.25
Dihedral (relative to mean thickness line), deg	0
Taper ratio (theoretical tip chord/root chord)	0.22
Airfoil section at root	NACA 63-009 mod.
Airfoil section at theoretical tip	NACA 63-009 mod.
Vertical tail:	
Area (included), sq ft	3.13
Span, ft	3.19
Aspect ratio	3.25
Sweepback of leading edge, deg	40
Sweepback of trailing edge, deg	6
Taper ratio (theoretical tip chord/root chord)	0.40
Airfoil section at root	NACA 63-009 mod.
Airfoil section at theoretical tip	NACA 63-009 mod.
Elevon:	
Total area (back of hinge line), sq ft	0.57
Chord (perpendicular to hinge line), ft	0.24
Total span, ft	1.32
Weight and balance:	
Weight, lb	199.2
Wing loading, lb/sq ft	31.59
Center-of-gravity position, percent $\bar{c}$	14.0
Moment of inertia in pitch, slug-ft^2	10.15
Duct:	
Inlet area of each duct, sq in.	2.75
Exit area of each duct, sq in.	1.77

[redacted]

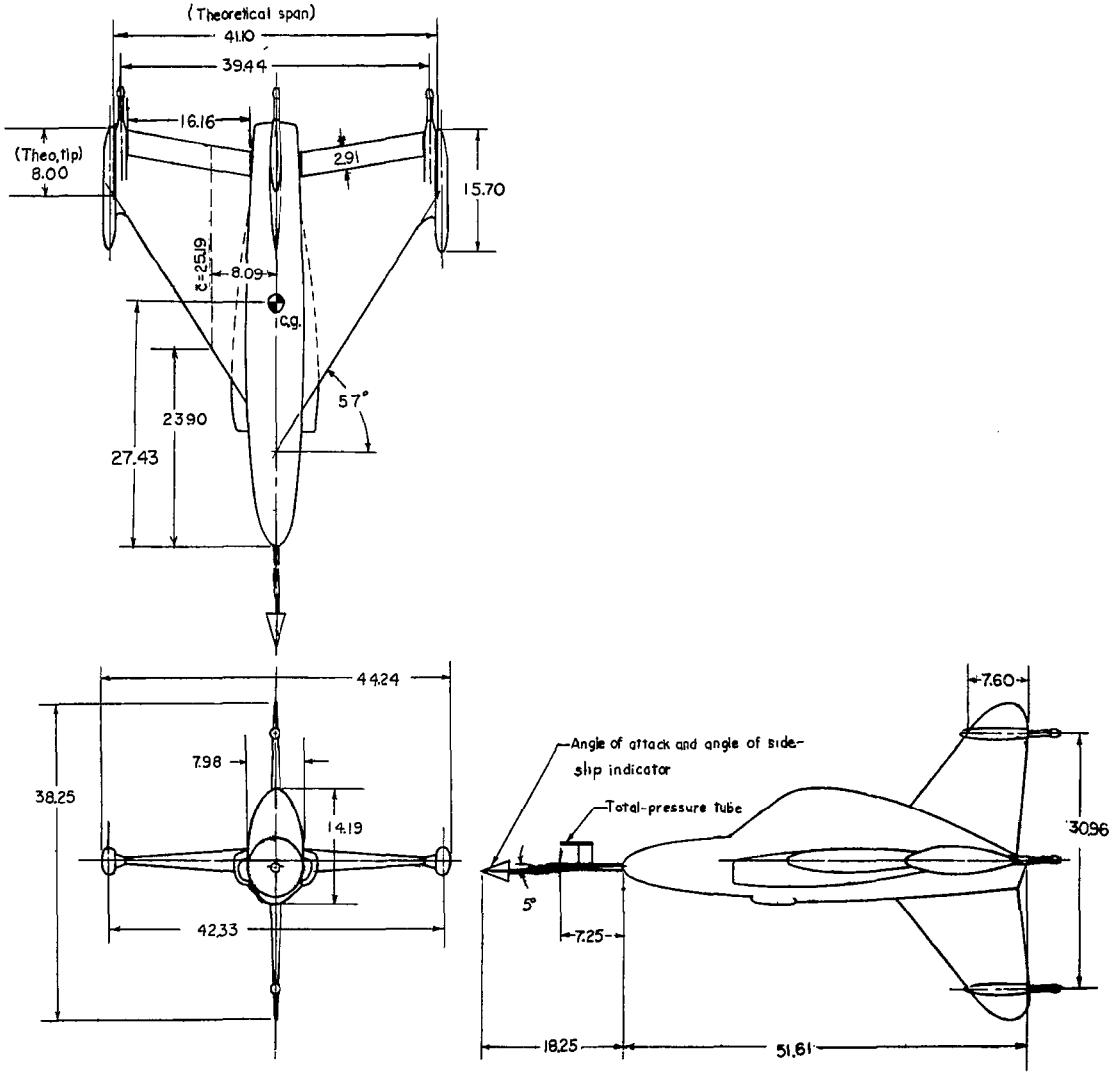

Figure 1.- Three-view drawing of the model. (All dimensions are in inches.)

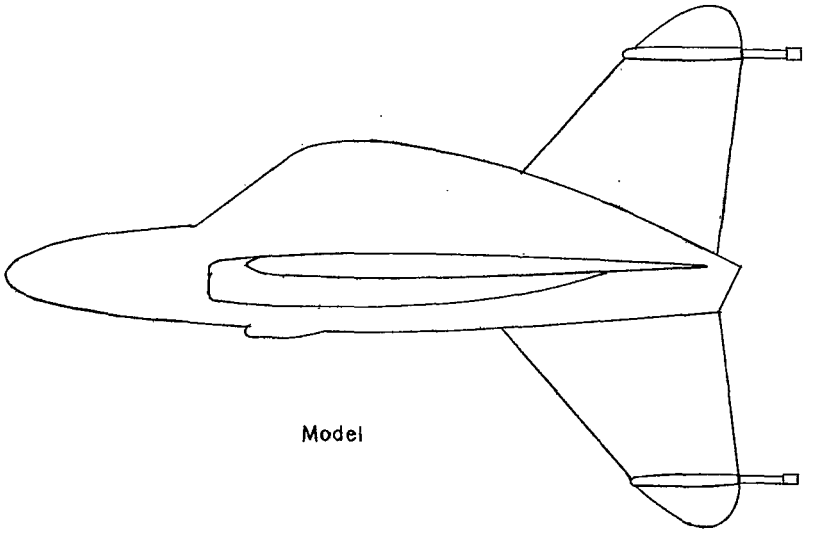

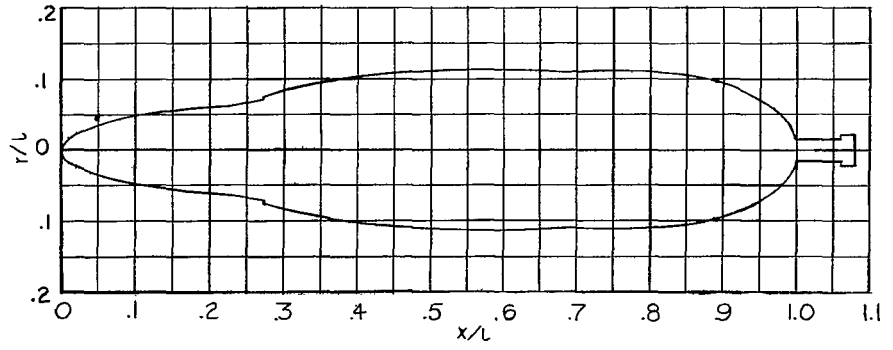

(a) Equivalent body of revolution.

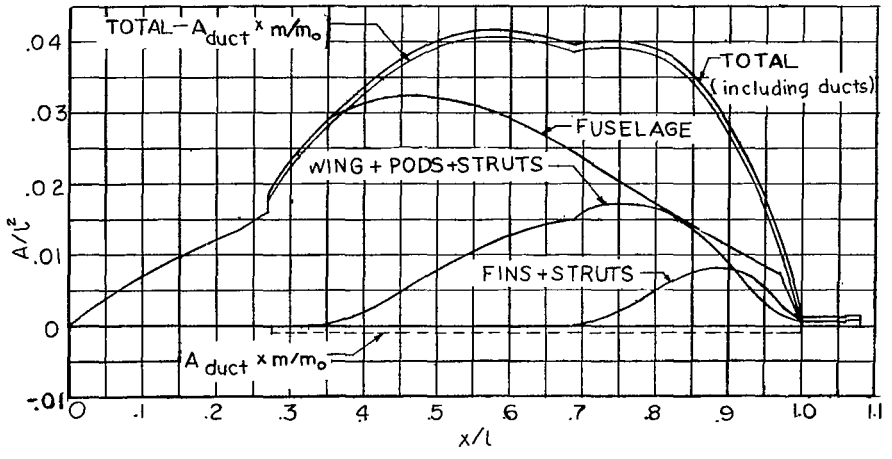

(b) Area distribution.

Figure 2.- Area distribution and equivalent body of revolution of the model.

L-80375

Figure 3.- Photograph of the model.

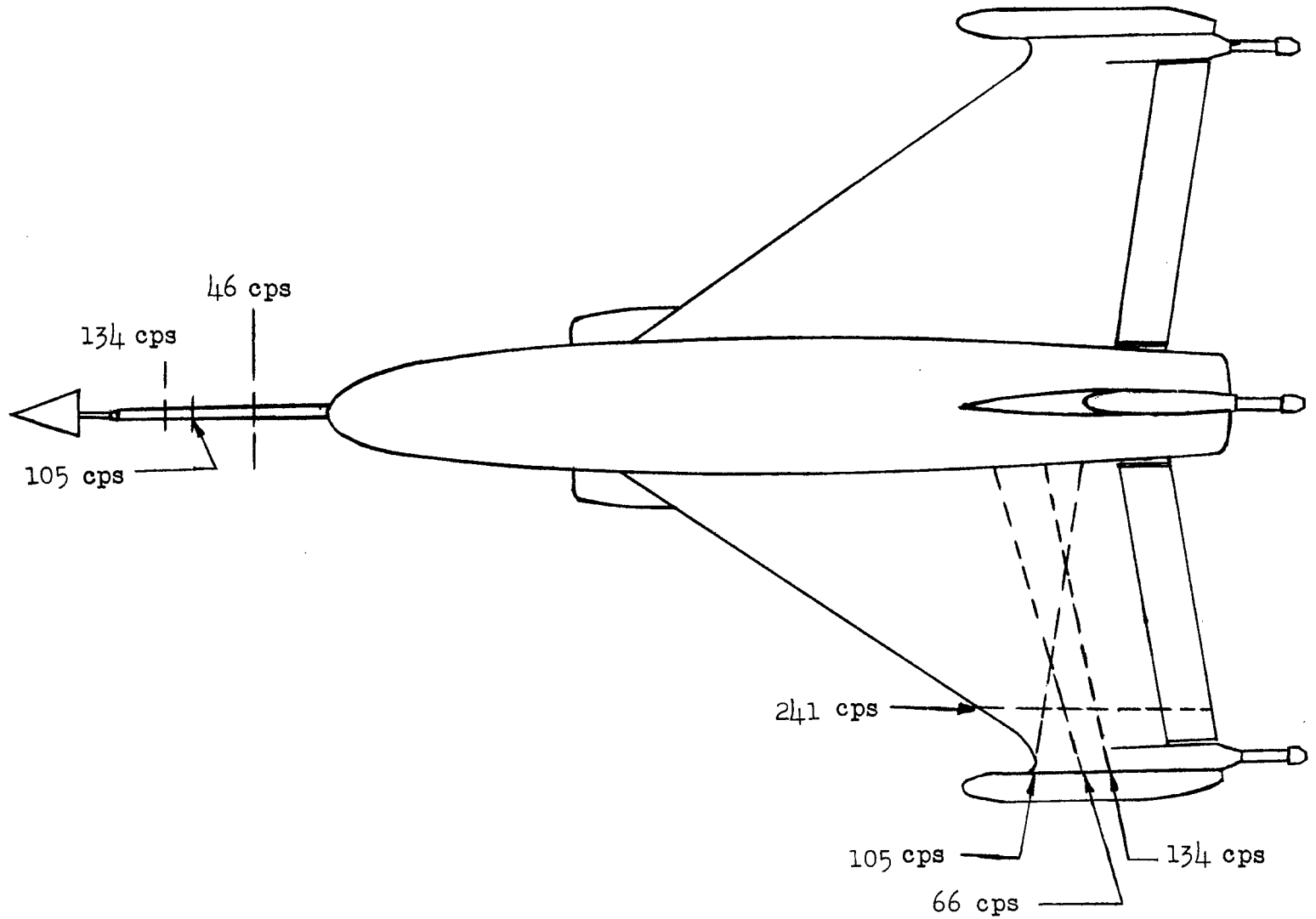

Figure 4.- Node lines at various shaking frequencies.

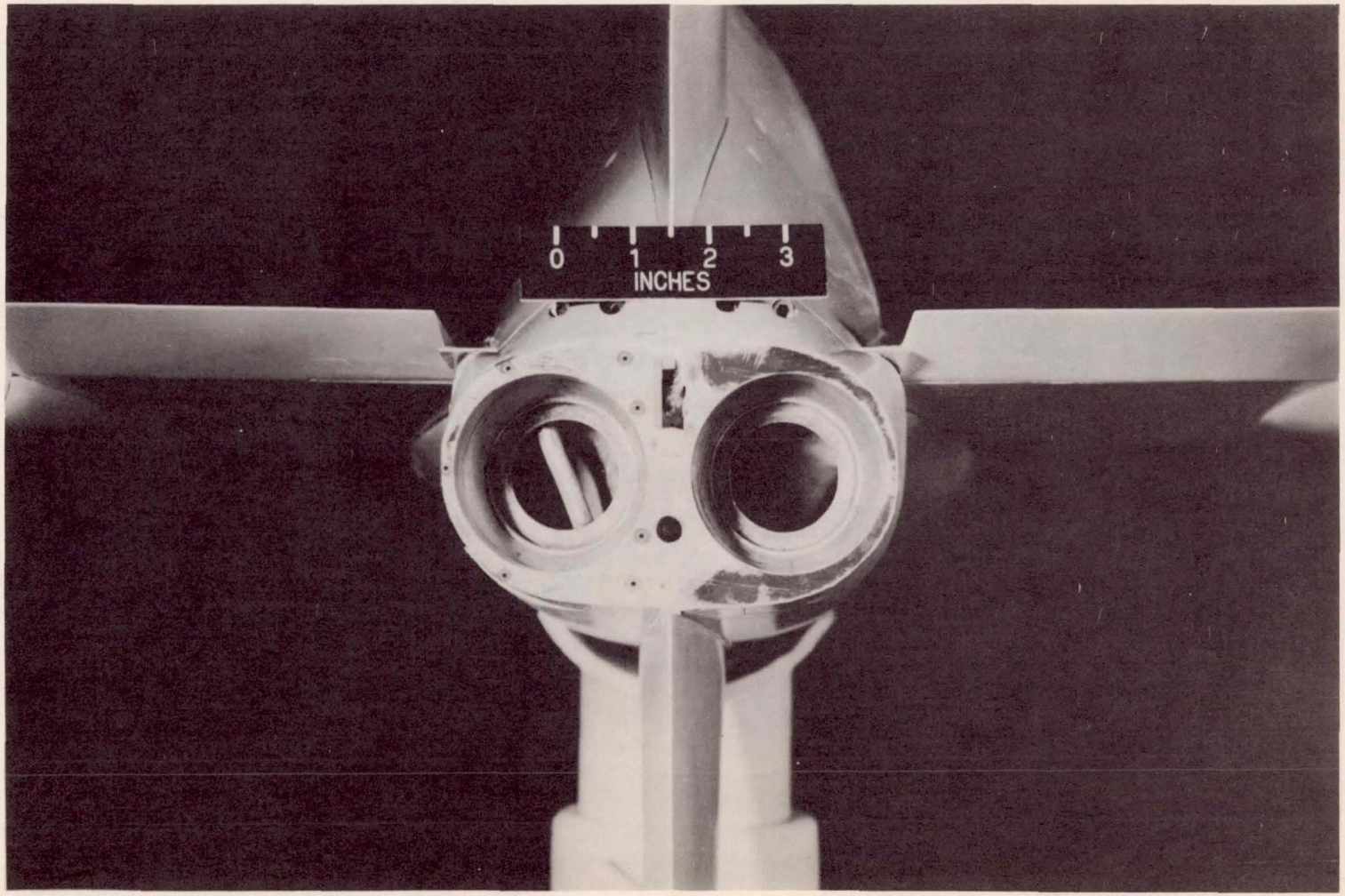

L-80373

Figure 5.- Base of the model.

L-80369

Figure 6.- Booster-model combination on the launcher.

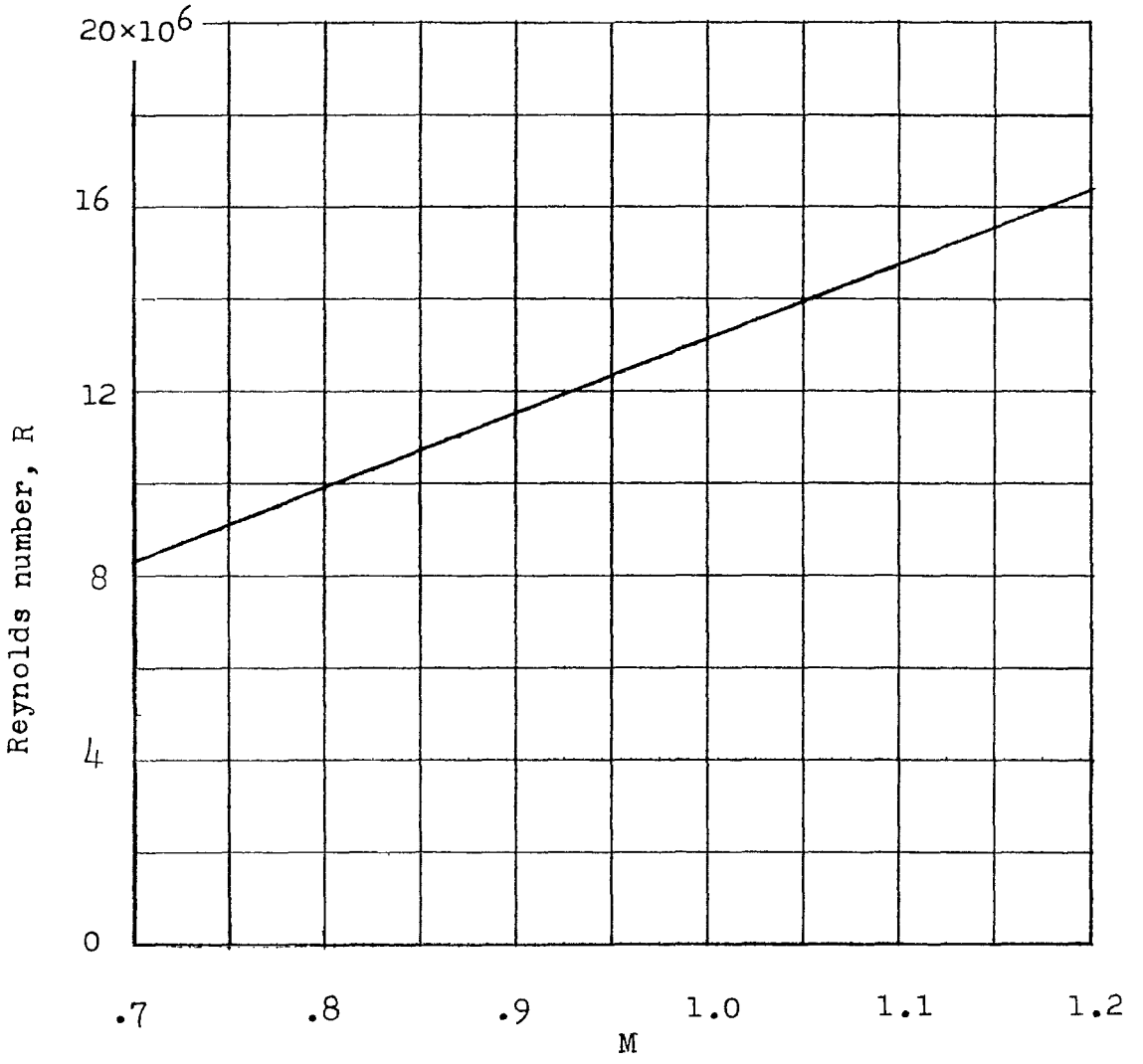

Figure 7.- Reynolds number as a function of Mach number.

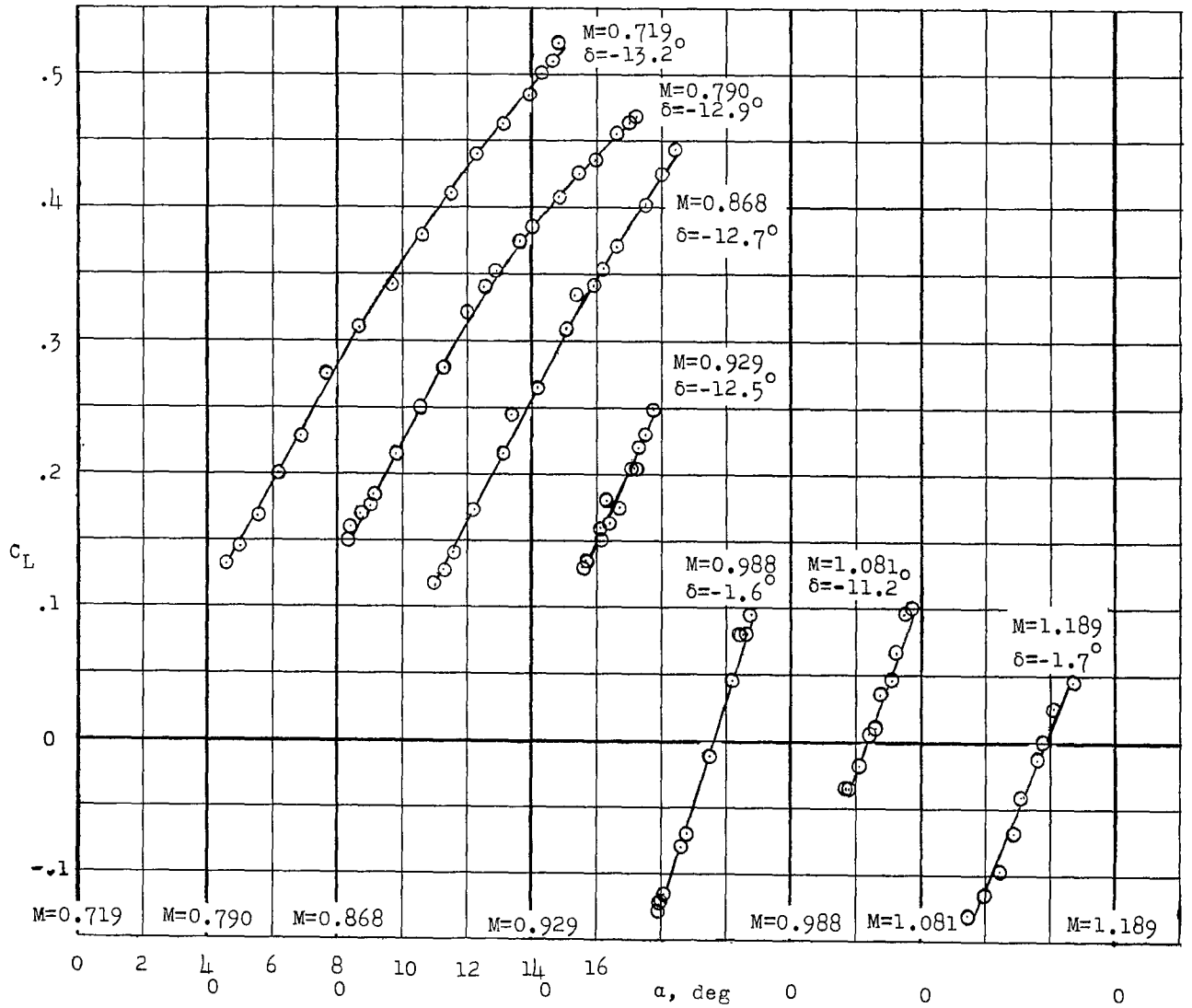

Figure 8.- The effect of angle of attack on lift for several oscillations.

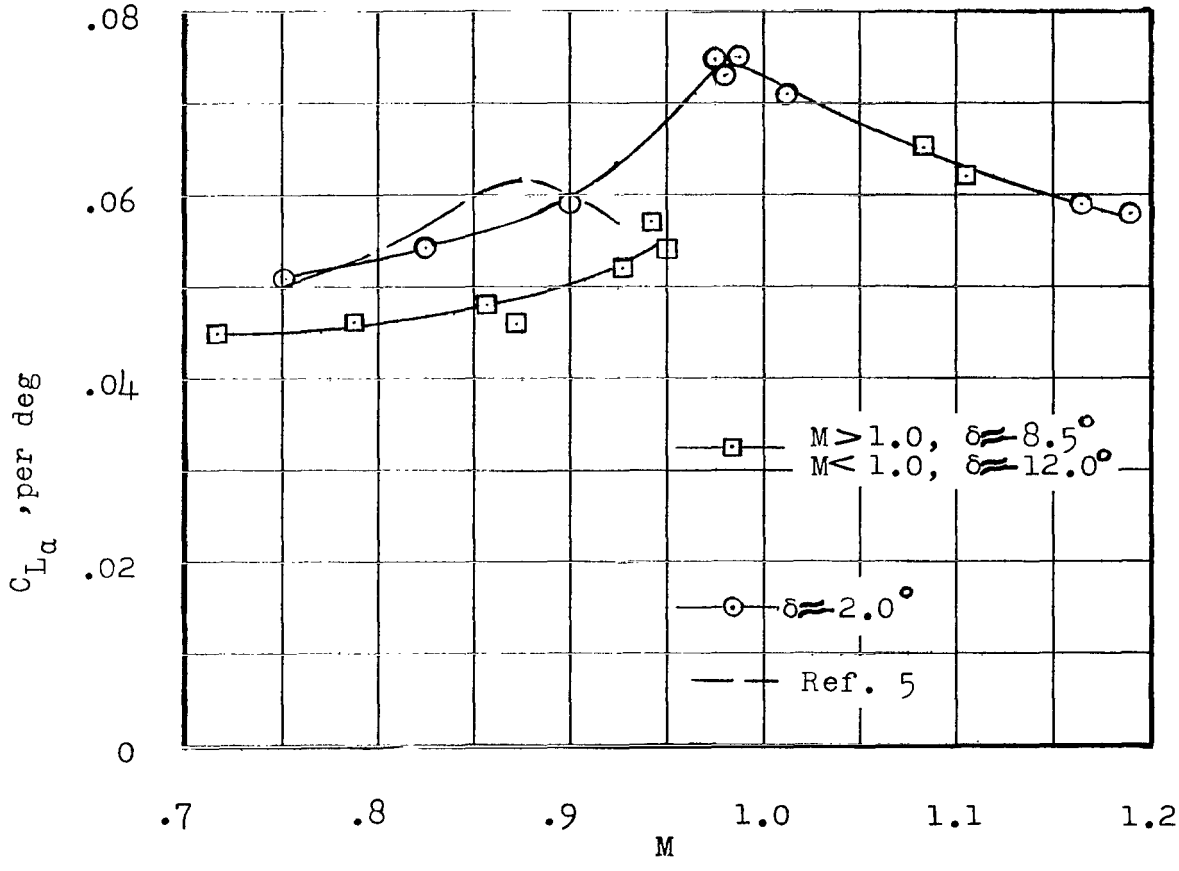

Figure 9.- Variation of lift-curve slope with Mach number.

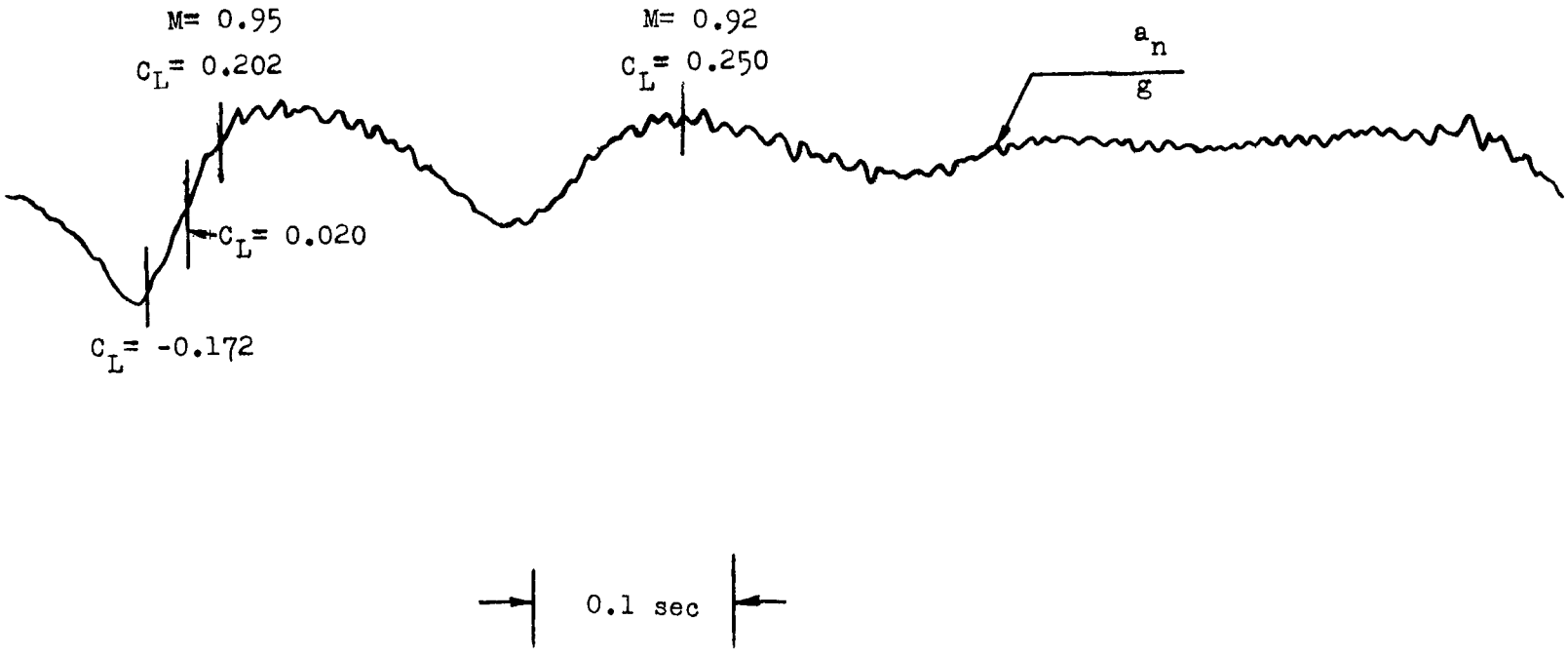

Figure 10.- Section of the telemeter record showing buffet.

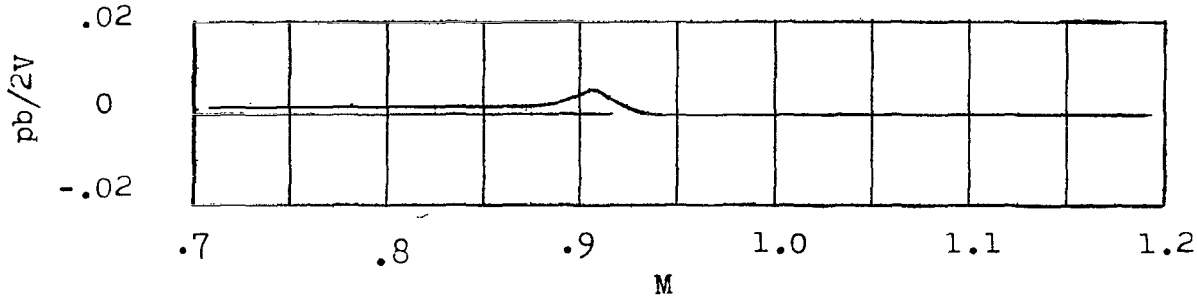

Figure 11.- Wing-tip helix angle.

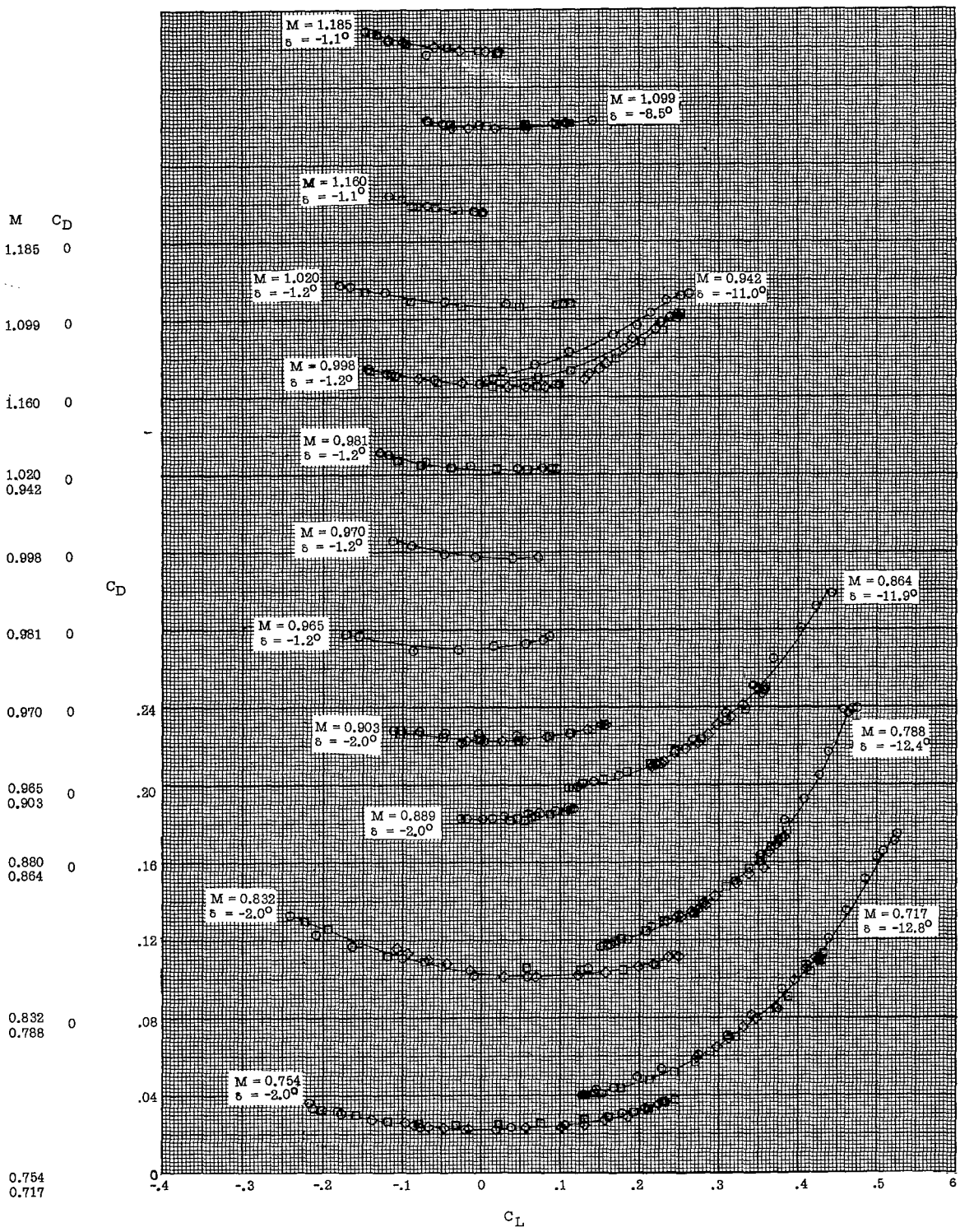

Figure 12.- Variation of drag coefficient with lift coefficient.

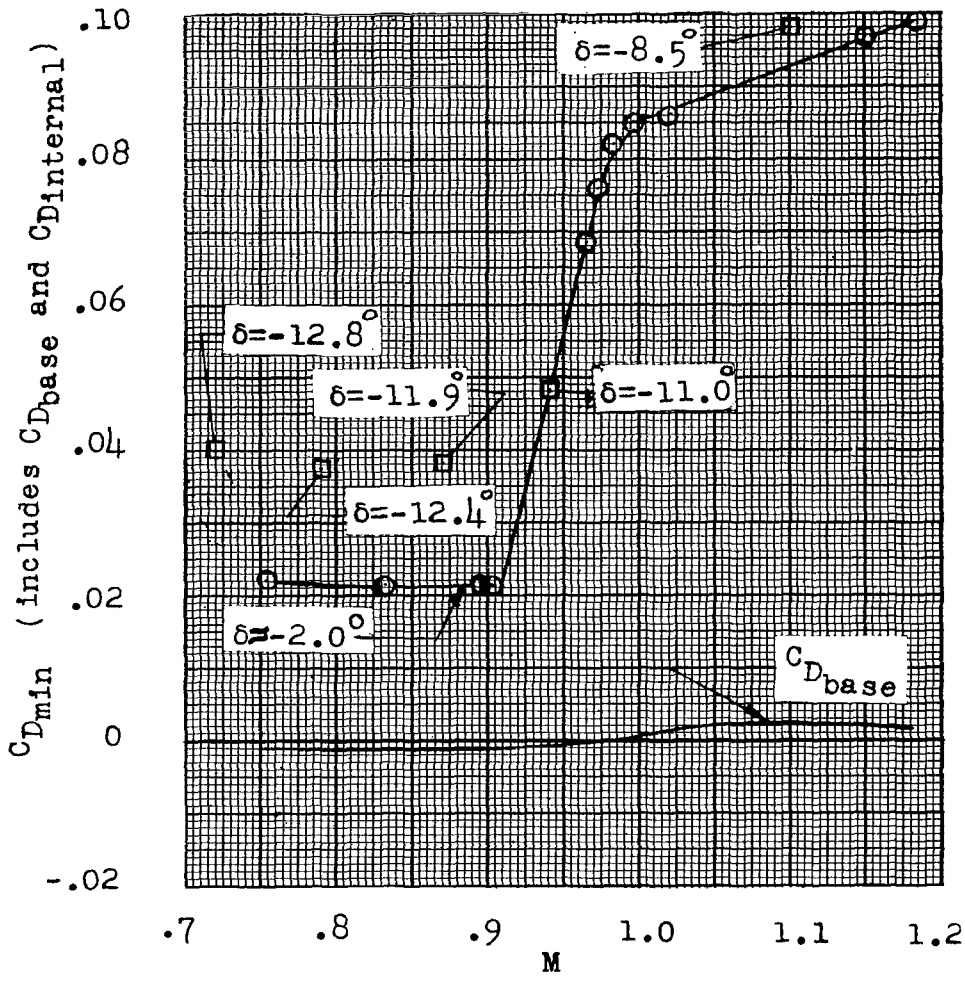

Figure 13.- Minimum and base drag coefficients.

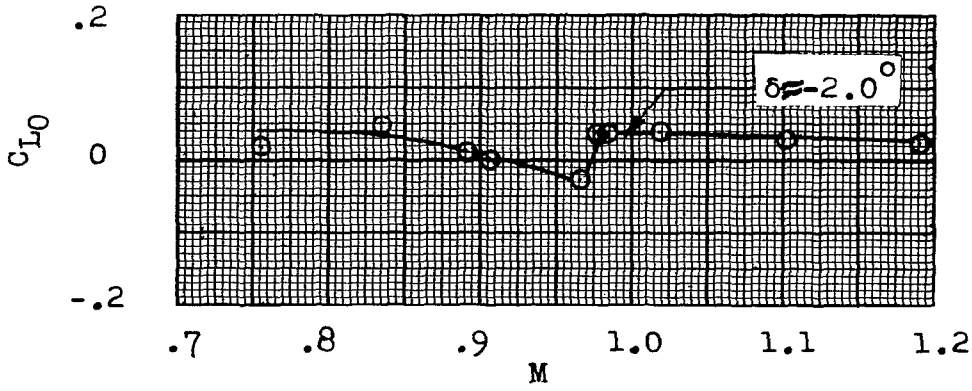

Figure 14.- Lift coefficient for minimum drag.

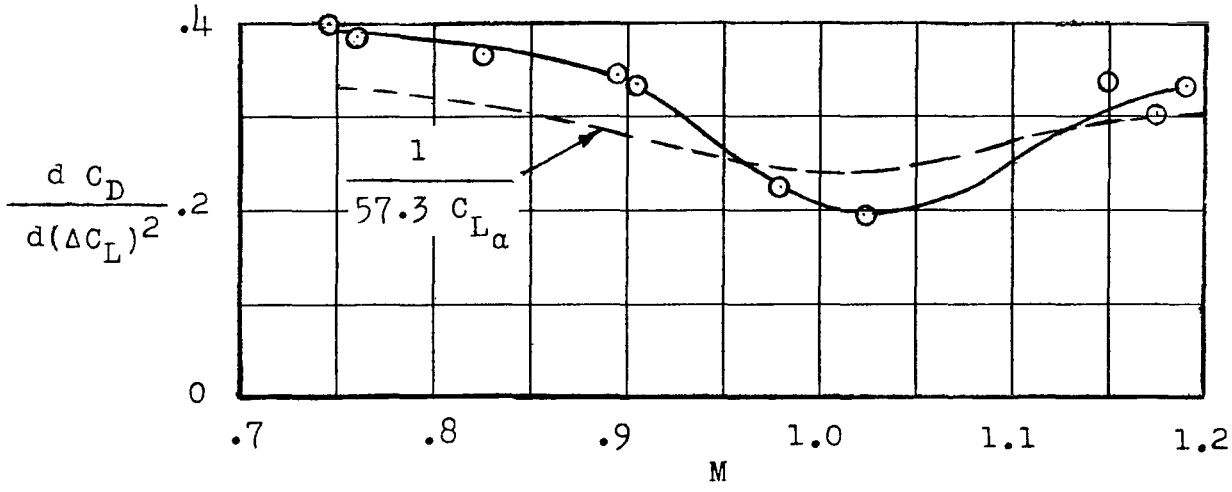

Figure 15.- The variation of drag parameter $dC_D/dC_L{}^2$ with Mach number at low lift.

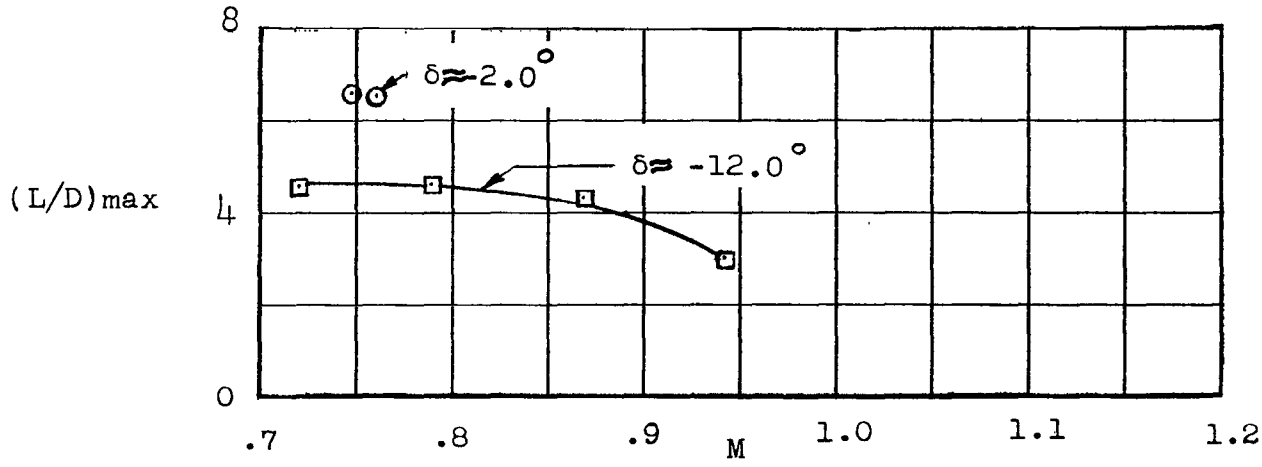

(a) Maximum lift-drag ratios.

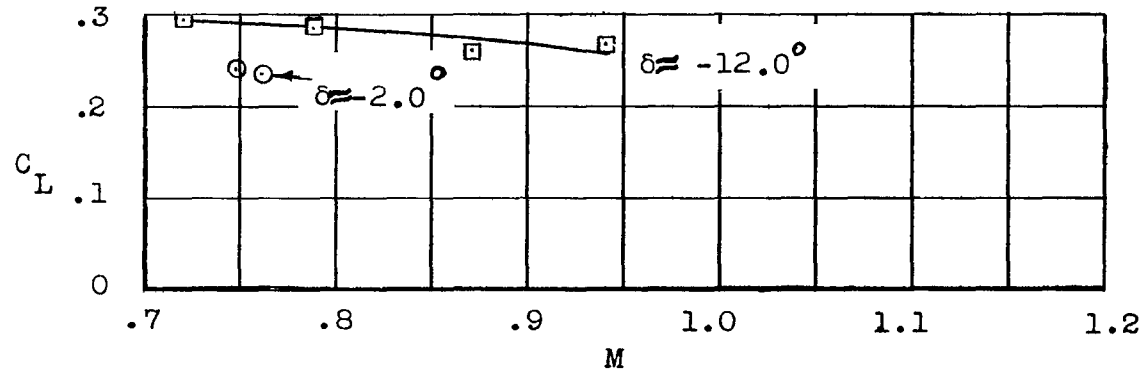

(b) Lift coefficient for maximum lift-drag ratio.

Figure 16.- Maximum lift-drag ratio and the lift coefficient for $(L/D)_{max}$.

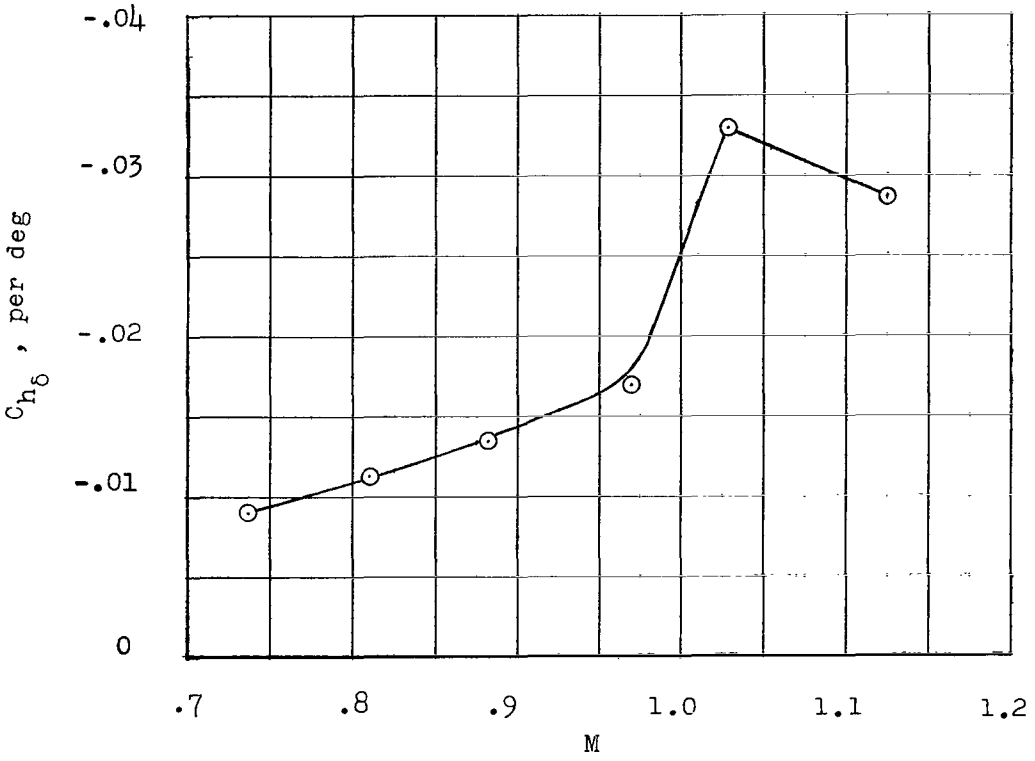

Figure 17.- Effect of Mach number on C_{h_δ}.

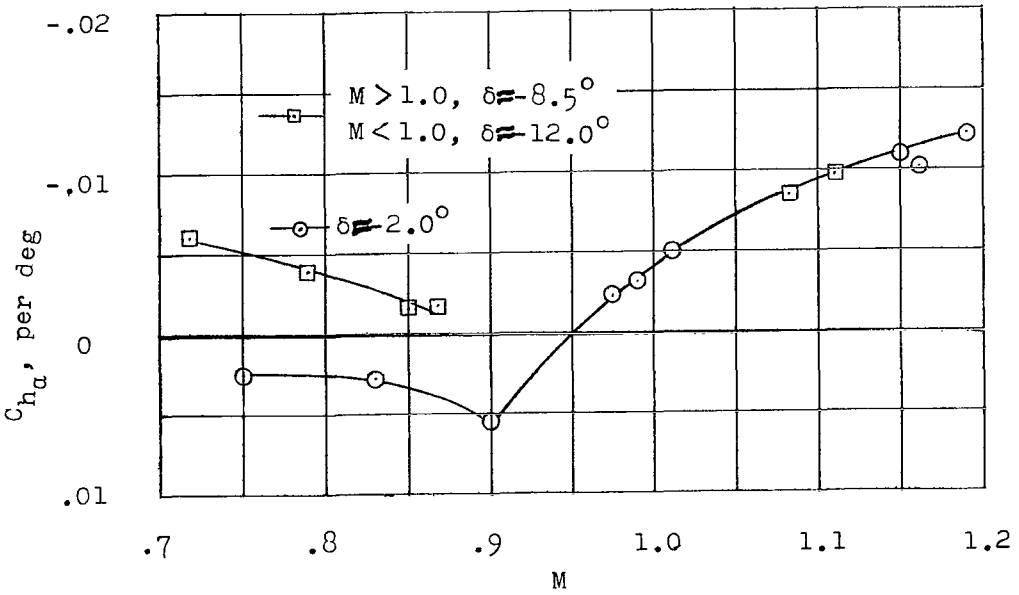

Figure 18.- Effect of Mach number on C_{h_α}.

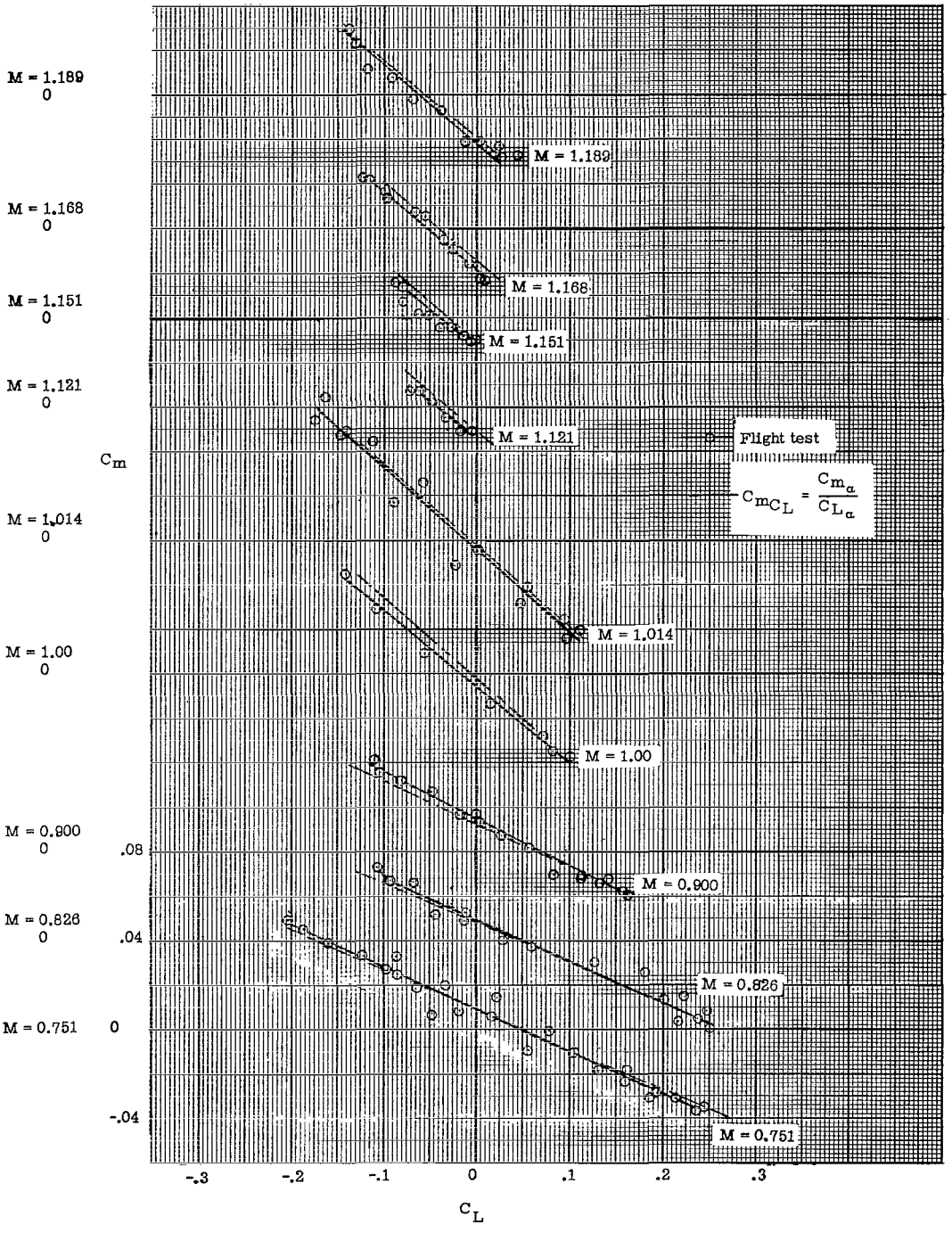

(a) $\delta \approx -2^\circ$.

Figure 19.- Pitching-moment coefficient as a function of lift coefficient for various Mach numbers. Center of gravity at $0.14\bar{c}$.

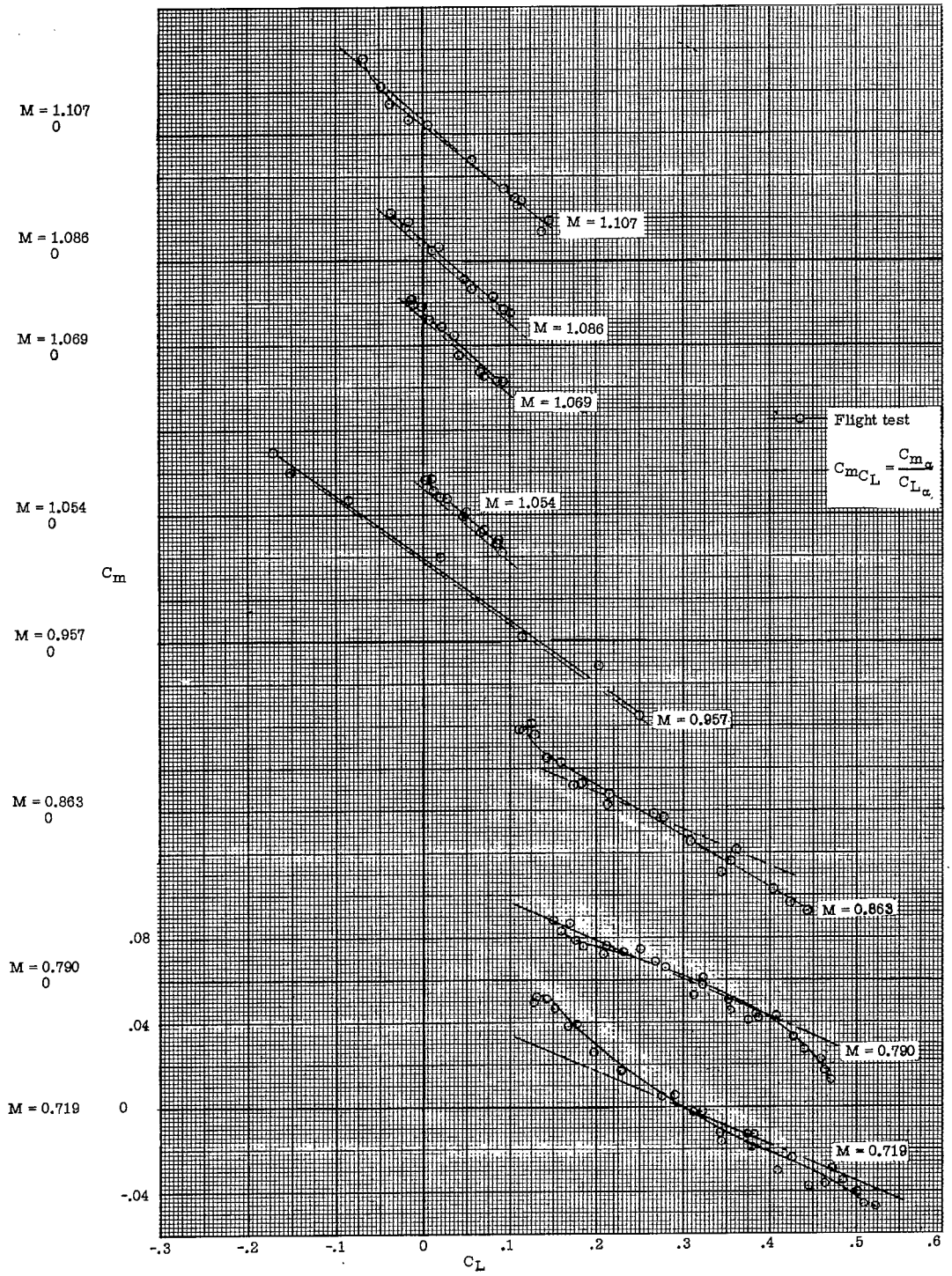

(b) $M > 1.0$; $\delta \approx -8.5^\circ$; $M < 1.0$; $\delta \approx -12^\circ$.

Figure 19.- Concluded.

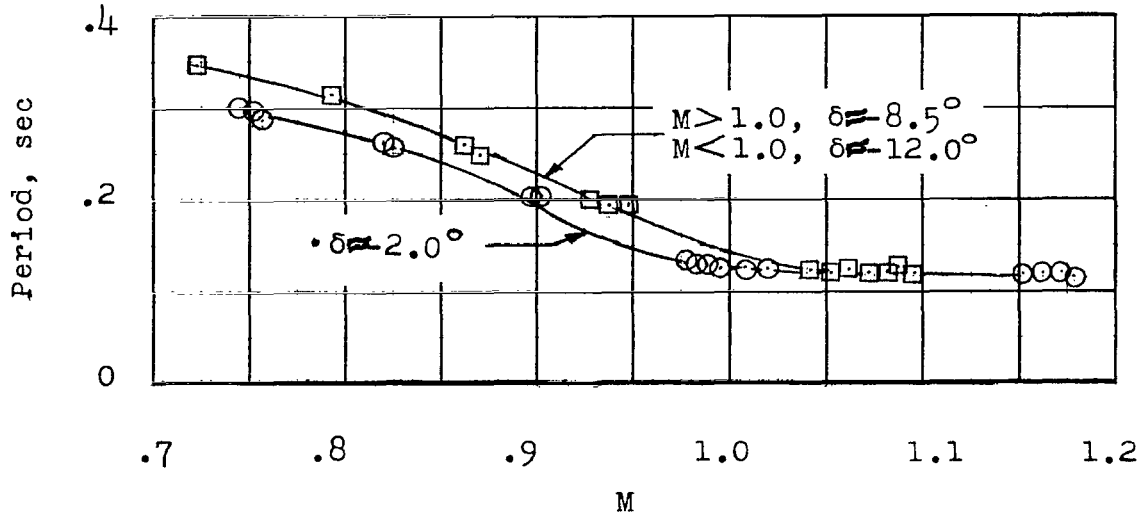

Figure 20.- Period of the longitudinal oscillation.

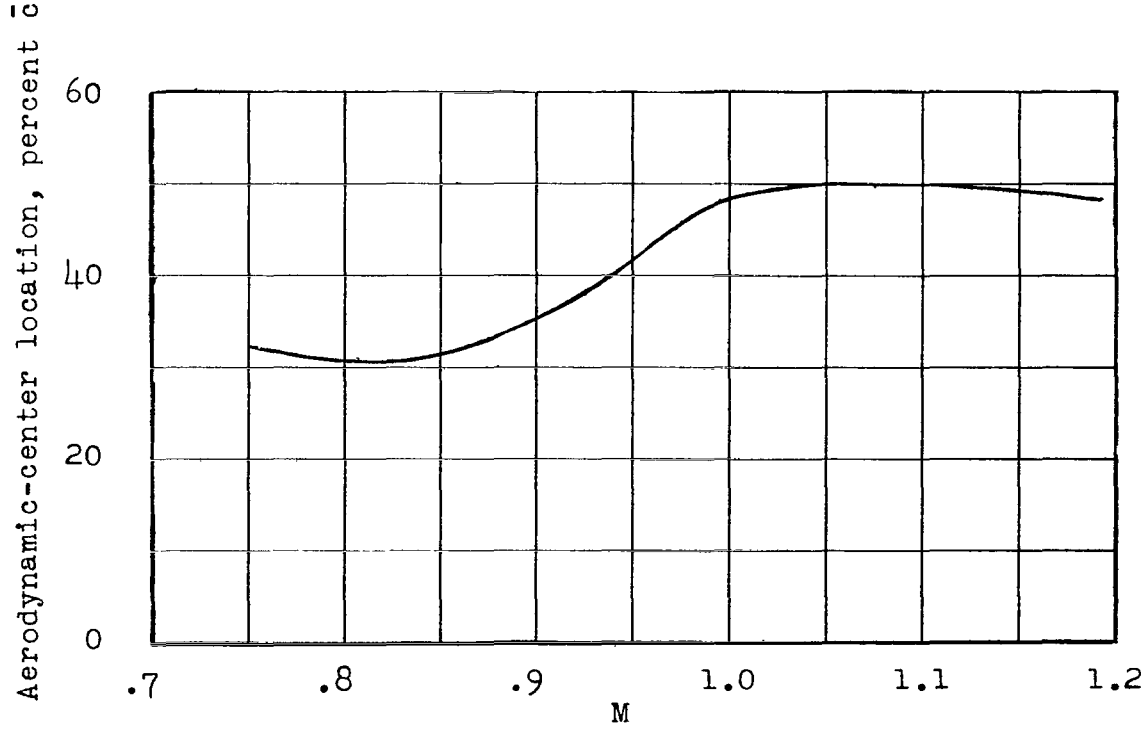

Figure 21.- Aerodynamic-center location for $\delta \approx -2.0^{\circ}$.

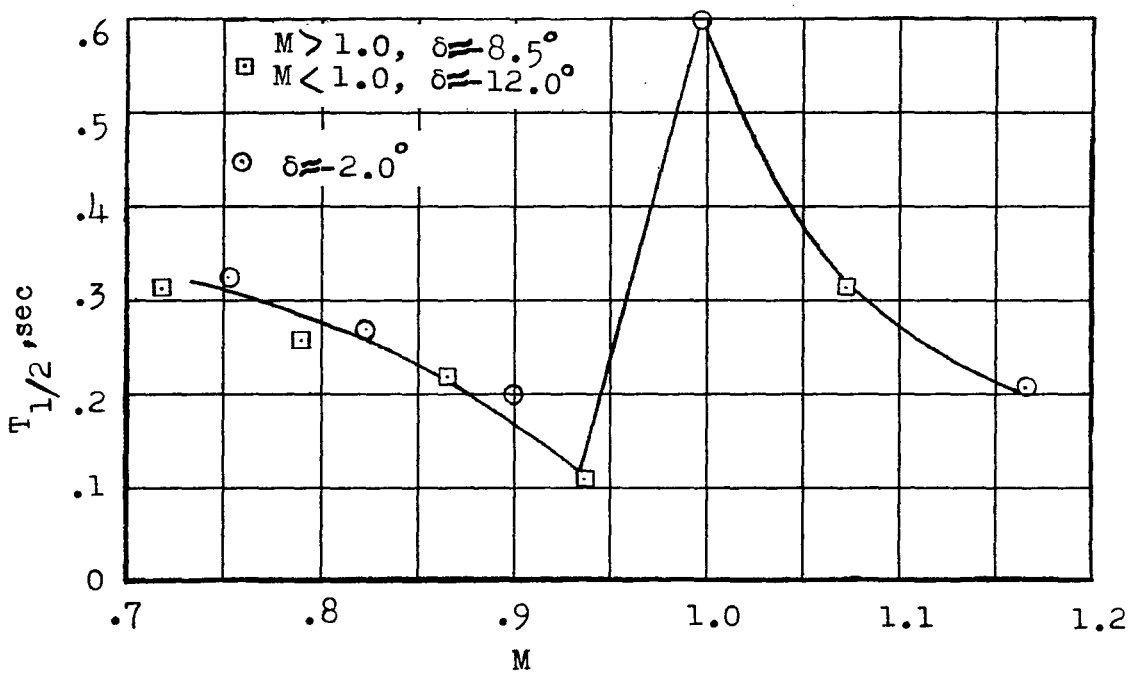

Figure 22.- Time to damp to half amplitude.

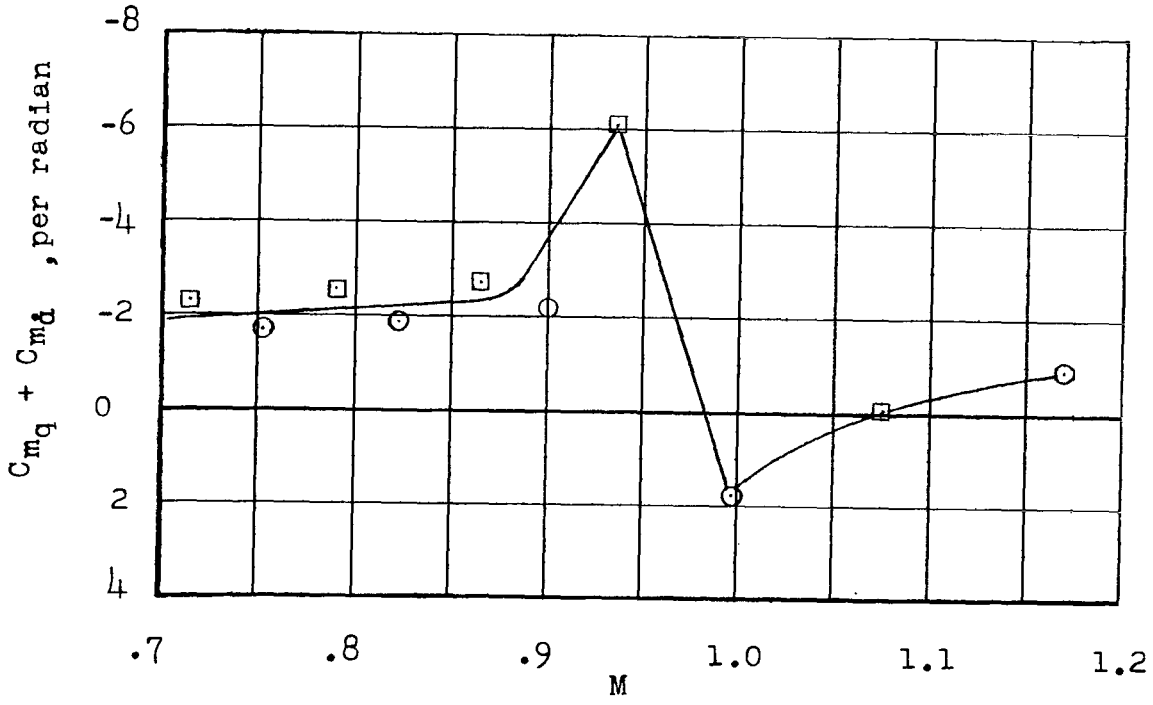

Figure 23.- Pitch-damping parameter. Center of gravity at $0.14\bar{c}$.

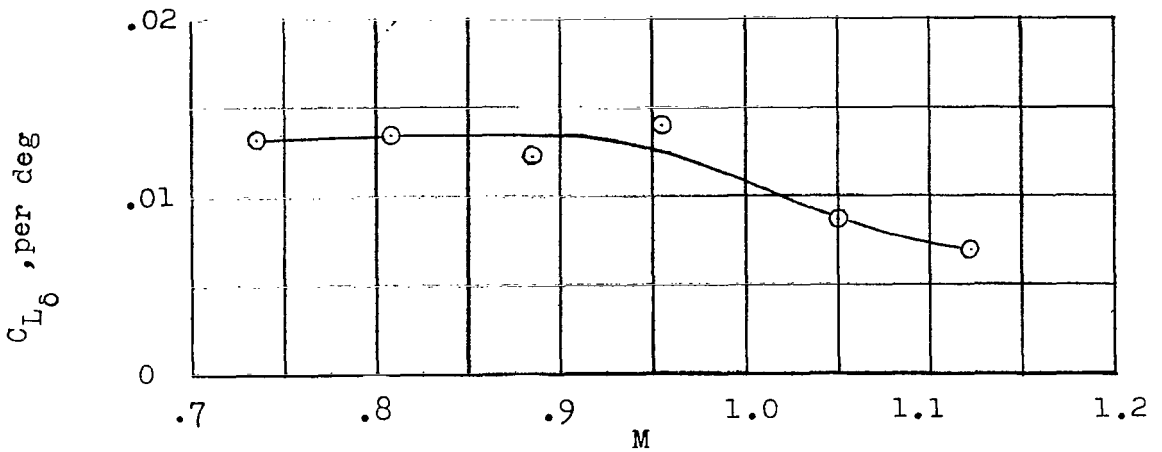

Figure 24.- Control lift effectiveness.

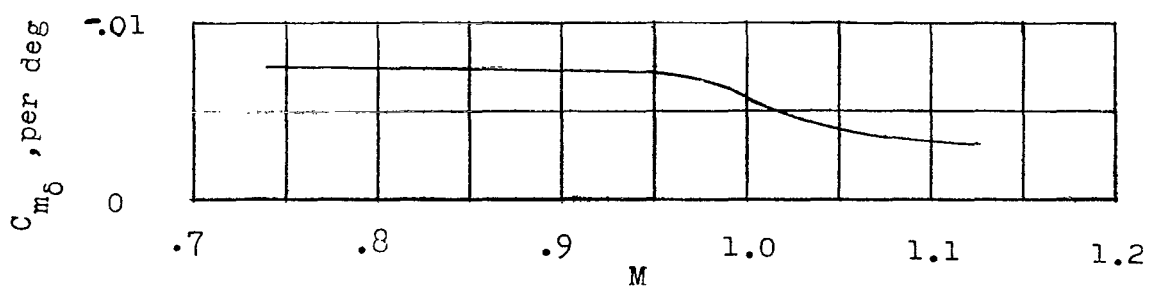

Figure 25.- Control pitching effectiveness. Center of gravity at 0.14$\bar{c}$.

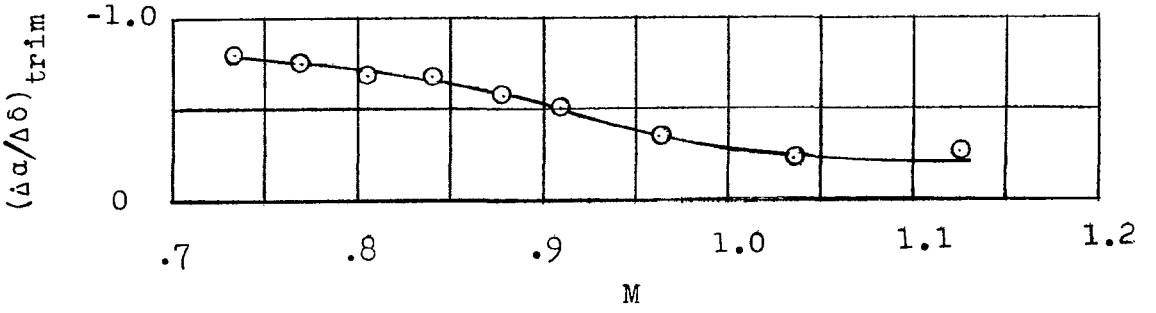

Figure 26.- Change in trim angle of attack per degree of elevon deflection.

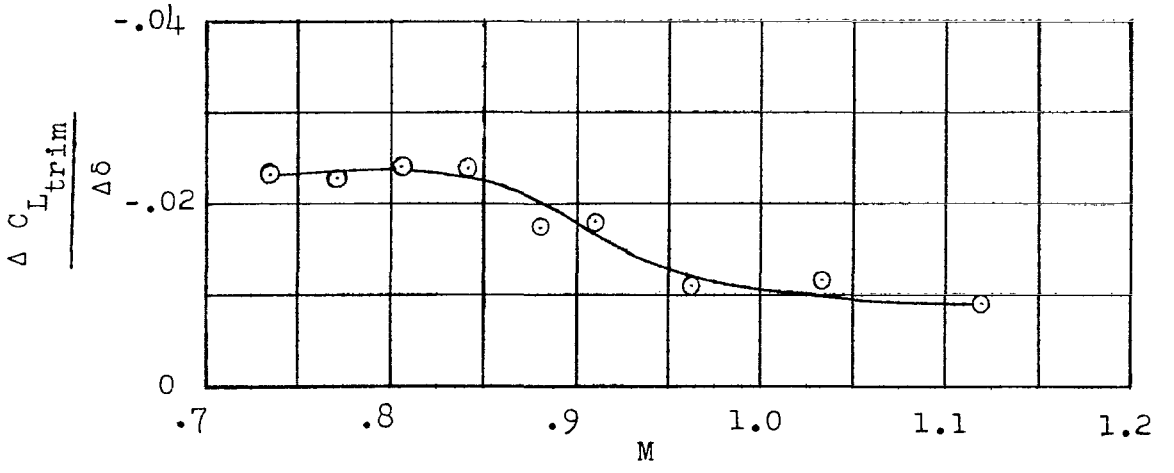

Figure 27.- Trim lift coefficient per degree elevon deflection.

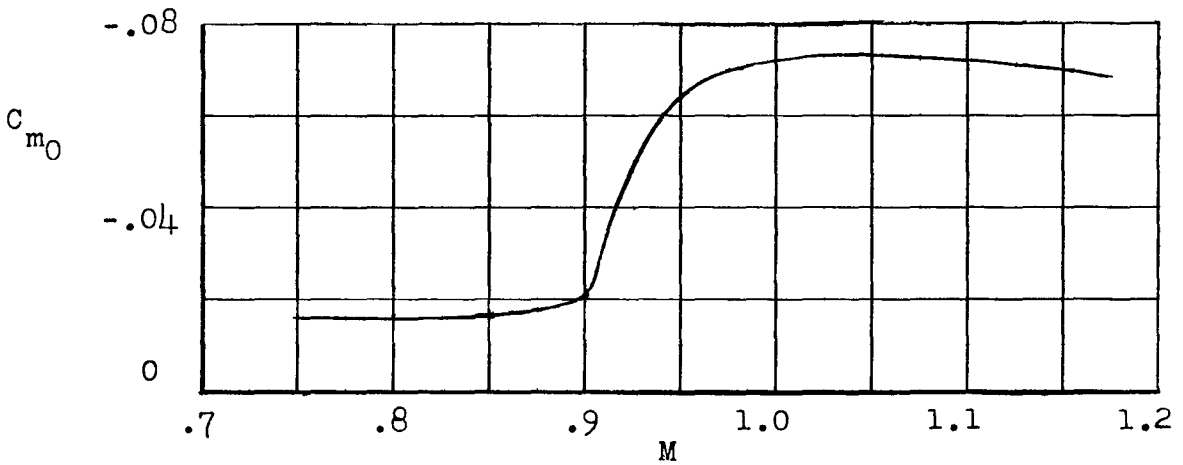

Figure 28.- Basic pitching-moment coefficient.